Long-Wavelength Quantum-Dot Infrared Photodetectors With Operating Temperature Over 200 K

Hong-Shi Ling, Shiang-Yu Wang, Chien-Ping Lee, *Fellow, IEEE*, and Ming-Cheng Lo

***Abstract*—We demonstrate the high-temperature operation of confinement enhanced dots-in-a-well (CE-DWELL) quantum-dot infrared photodetectors (QDIPs). The thin $Al_{0.3}Ga_{0.7}As$ barrier layer added above the InAs QDs greatly improve the lateral confinement of QD states in the $In_{0.15}Ga_{0.85}As$ DWELL structure and the device performance. With better device parameters of CE-DWELL, it is possible to achieve high quantum efficiency, high operating temperature, and long-wavelength detection at the same time.**

***Index Terms*—Infrared detectors, photodetectors, quantum dots (QDs), quantum effect semiconductor devices.**

LONG-WAVELENGTH (8–12 μm) infrared (LWIR) detectors are essential to the thermal radiation detection of room-temperature objects. Recent results in quantum-dot infrared photodetectors (QDIPs) have shown great potential in such applications with low cost and high operating temperatures [1]–[13]. Although encouraging results have been demonstrated with operating temperatures over 200 K [4], [5] and even up to room temperature [6], [7], the detection wavelengths of these devices are out of the LWIR atmospheric transmission window. Unfortunately, it is not trivial to adjust the QDIP's detection band due to the limitation of the self-assembled growth process of QDs. In order to fit the detection band into the LWIR window, many efforts have been focused on the QDIPs with dots-in-a-well (DWELL) structures [9]–[13]. The additional quantum wells in the DWELL structure provide the flexibility in tuning the detection wavelength. Based on such an idea, DWELL QDIPs working at 9.9 μm with elevated operating temperature (190 K) have been demonstrated recently [12]. However, the performance of DWELL QDIPs is still restricted because of the poor quantum efficiency. To solve this problem, we have recently developed a new structure, which uses a thin AlGaAs layer on InAs QDs in the DWELL structure to provide enhanced electron confinement in the QDs. With this structure, the quantum efficiency and responsivity are greatly enhanced by an order of magnitude [13].

In this letter, we further improved the confinement enhanced DWELL (CE-DWELL) structure by optimizing the device structure. Two devices with different confinement enhancing layers are compared. The device performance at different temperatures for the two devices was investigated. Despite dramatic difference in the device characteristics, both devices can be operated at temperatures higher than 200 K.

The samples were grown by a Veeco GEN-II molecular beam epitaxy system on (001) semi-insulating GaAs substrates. In each sample, the active region contains ten layers of CE-DWELL structure separated by 72-nm GaAs barrier layers and is sandwiched between two 500-nm n+ GaAs contact layers. Compared to our previous result [13], thicker GaAs barriers were used. The thicker GaAs barriers can provide longer acceleration path for the excited carrier to enhance the current gain [4]. The growth temperature was kept at 510 °C for the whole active region. 2.4 MLs of InAs QD layer was deposited on a 2-nm $In_{0.15}Ga_{0.85}As$ layer and covered by $Al_{0.3}Ga_{0.7}As$–$In_{0.15}Ga_{0.85}As$ structure to comprise the CE-DWELL unit. The total thickness of the CE-DWELL structure was kept at 8 nm. A Si δ-doped layer with a concentration of 2×10^{10} cm^{-2} was inserted 2 nm under each QD layer. For sample A, 2 nm of $Al_{0.3}Ga_{0.7}As$ confinement enhancing layer was used, while the thickness of $Al_{0.3}Ga_{0.7}As$ layer is 3 nm in sample B. The thickness of the AlGaAs layer in sample A was chosen so that it covers only the sidewalls of the QDs. On the other hand, in sample B, the QDs were fully covered by the AlGaAs layer. Fig. 1 shows the transmission electron microscope (TEM) images of the test samples with different AlGaAs layer thickness. It confirms the coverage of AlGaAs on the QDs are different in the two samples. The effect of the AlGaAs layer thickness on the carrier confinement was verified by the photoluminescence measurement. The ground state energy of sample B is about 27 meV higher than that of sample A due to the better quantum confinement from the thicker AlGaAs layer.

Standard processing techniques were then applied for the device fabrication. 260×370 μm^2 mesas with AuGe contact rings were formed to allow normal incidence measurement from the mesa top. In all measurements, the bottom contact is referred as ground. The photocurrent spectra were measured by a Fourier transform infrared spectrometer and the absolute responsivity was calibrated by a 1273 K blackbody radiation source with lock-in techniques. A Ge wafer was inserted in the optical path to filter out photons with wavelength shorter than 2 μm.

Manuscript received September 09, 2008; revised October 30, 2008. First published December 09, 2008; current version published January 14, 2009.

H.-S. Ling, C.-P. Lee, and M.-C. Lo are with the Department of Electrical Engineering, National Chiao Tung University, Hsinchu 300, Taiwan (e-mail: karshe.ee92g@nctu.edu.tw; cplee@mail.nctu.edu.tw; mclo.ee91g@nctu.edu.tw).

S.-Y. Wang is with the Institute of Astronomy and Astrophysics, Academia Sinica, Taipei 106, Taiwan (e-mail: sywang@asiaa.sinica.edu.tw).

Color versions of one or more of the figures in this letter are available online at http://ieeexplore.ieee.org.

Digital Object Identifier 10.1109/LPT.2008.2009130

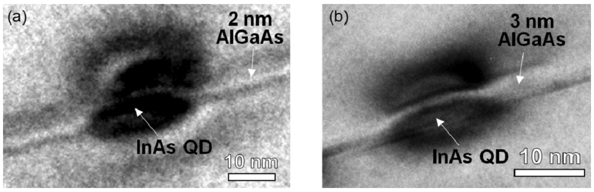

Fig. 1. TEM images of the samples with (a) 2-nm AlGaAs and (b) 3-nm AlGaAs layer on the QDs.

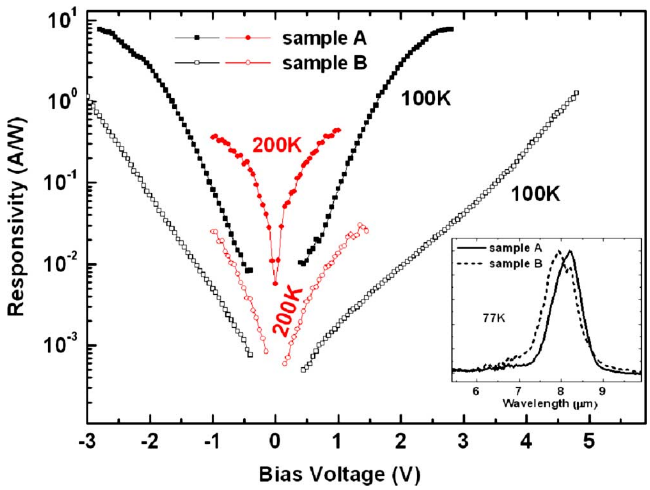

Fig. 2. Voltage dependence of the peak responsivity of the two samples at 100 K and 200 K. The insert shows the responsivity spectra of the two samples at -0.35 V and 77 K.

Fig. 2 shows the photocurrent spectra of the two samples and the bias dependent responsivity curves at 100 K and 200 K. Both samples reveal suitable response band for LWIR detection. The response peak of sample A is at 8.2 μm, while for sample B, it is slightly shorter, at about 8 μm. The thicker AlGaAs layer in sample B pushed the response peak toward short wavelength as expected. For comparison, DWELL QDIPs without the AlGaAs layer show a peak responsivity at 9.2 μm [13]. The relatively narrow bandwidth of the photocurrent spectrum ($\Delta\lambda/\lambda p \sim 10\%$) suggests that bound-to-bound transitions in the QDs are responsible for the optical absorption in both samples. Comparing the responsivity of the two samples, sample A shows higher reponsivity at both temperatures. At 200 K, it reaches 0.37 A/W at 0.8 V. Although there is a stronger confinement effect in sample B, because of thicker AlGaAs layers, the responsivity instead degraded. However, the responsivity of sample B (4.9 mA/W at -1 V and 100 K) is still comparable to the responsivity of the sample without the AlGaAs layer (8 mA/W at the same electric field and 100 K) [13].

To understand the origin of the inferior responsivity in sample B, the current gain was examined with the noise measurement [3]. The obtained current gain of the two devices as a function of bias voltages at 100 K and 200 K are shown in Fig. 3. Clear degradation of current gain is shown in sample B due to the thicker AlGaAs layers. Furthermore, the two samples show distinct gain behaviors. The current gain of sample B possesses a clear asymmetry between the positive bias and the negative bias. Because of thicker AlGaAs layers used, the QDs in sample

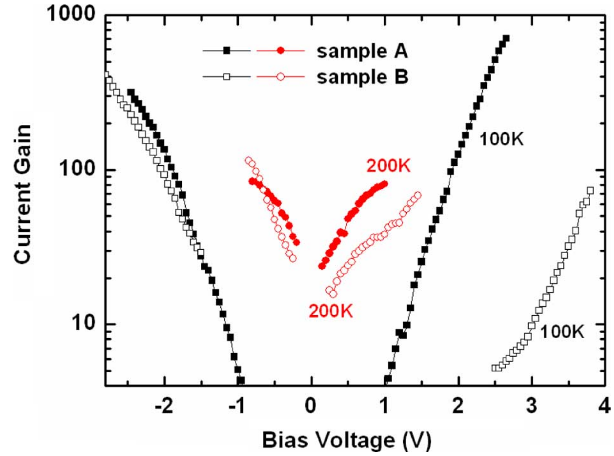

Fig. 3. Current gain curves of the two samples at 100 K and 200 K.

B are fully covered. When positively biased, the photogenerated electrons have to overcome the potential barrier of AlGaAs and pass through the InGaAs well. The capture probability of the excited carriers into the adjacent InGaAs well is high when the bias is low. Higher positive voltages are needed to reach the same current gain as that in the reverse bias. On the other hand, in sample A, because of thinner AlGaAs layers, the current gain is more symmetric under different bias polarities and it has a much higher gain than that of sample B under the same positive bias. The current gain difference of the two samples also depends on the device temperature. At higher temperatures, because of the additional thermal energy, the capture probability of electrons decreases in both bias polarities. The gain increases in both samples and the asymmetry reduces in sample B. Compared to our previous result [13], the current gain in sample A is about 5 times higher as expected, showing the advantage of thicker GaAs barrier.

The decrease of responsivity in sample B cannot be only explained by the gain degradation, since the current gain of the two samples is similar under negative biases. This implies the quantum efficiency of sample B is also degraded. To further investigate the quantum efficiency, the polarization-dependent photoresponse of our devices was measured using the 45° edge coupling scheme. For sample A, the response for the radiation with the electric field parallel to the epilayers (transverse-electric (TE) response) is $\sim$42% of the response for the radiation with the electric field perpendicular to the layers (transverse-magnetic (TM) response). For sample B, however, the TE to TM response ratio was only $\sim$25%. A stronger absorption or higher quantum efficiency is expected for sample A, when the radiation is normal to the surface of the detectors.

The better normal incident absorption (TE response) for sample A comes from a better lateral confinement of carriers in QDs. Because the AlGaAs barrier layer is thin enough to leave the tips of the QDs uncovered, this additional barrier is mainly in the lateral direction. This lateral confinement enhances normal incident absorption as quantum mechanics dictates for 3-D quantum structures. For sample B, because of the thick AlGaAs layer, the tips of the QDs are covered. Since the vertical confinement is also enhanced in this case, the advantage

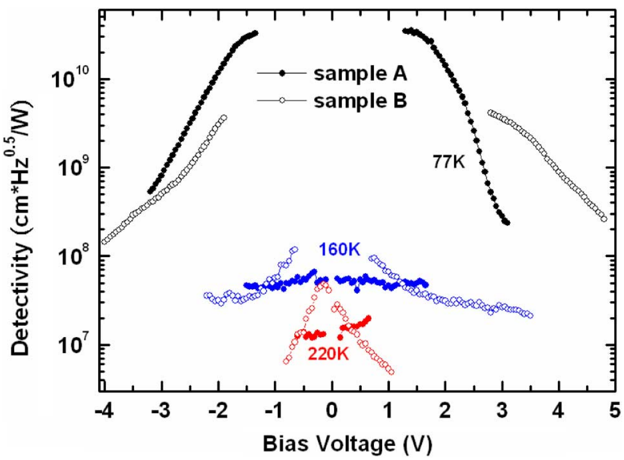

Fig. 4. Detectivity at different voltages of the two samples at 77 K, 160 K, and 220 K.

from the lateral confinement is reduced. This explains why the quantum efficiency of sample A is much better than that of sample B under normal incident configuration. This also shows the importance of having a proper AlGaAs layer thickness in the devices.

The AlGaAs layer in sample B, although too thick from the responsivity point of view, is effective to reduce the dark current. This is especially true at high temperatures and low bias voltages. The dark current density for sample A, sample B, and the sample without AlGaAs are 5.6×10^{-4} A/cm^2, 1.1×10^{-7} A/cm^2, and 2.0×10^{-4} A/cm^2, respectively, at 1 V and 100 K. The AlGaAs layers in sample B effectively block the low energy part of the dark current. So the detectivity of sample B is not necessarily worse compared with that of sample A. Fig. 4 shows the specific detectivity of the two samples at different temperatures. At 77 K, the highest measured detectivity for sample A is 3.56×10^{10} cm$\cdot$Hz$^{0.5}$/W at 1.4 V. This shows the superior performance of the CE-DWELL structure. However, as the temperature increases, sample B starts to show better performance. At 220 K, the highest detectivity measured for sample B is 4.85×10^{7} cm$\cdot$Hz$^{0.5}$/W at -0.15 V, which is about 2.4 times higher than that of sample A. When the temperature is raised to 240 K, the detectivity reaches 1.4×10^{7} cm$\cdot$Hz$^{0.5}$/W at -0.1 V for sample B, while the dark current is too high for sample A for the measurement. Furthermore, the BLIP temperature for sample B is about 140 K within 0.3 V which is 40 K higher than that of sample A. It should be also noticed that the performance of sample B could be further improved with the grating coupled configuration.

The comparison of two samples shows an important factor for the high temperature operation. Sample A is a typical high performance detector at 77 K with good carrier collection capability. However, as the temperature increases, the superior carrier transport property induces high dark current which is not acceptable in real applications. On the other hand, although the insertion of the thicker AlGaAs layer in sample B degrades the responsivity, the dark current is suppressed even more especially at small biases. As the temperature increases, the thermal energy helps the photocarrier collection and provides a better performance at higher temperatures. This indicates the importance of the current suppression for the high operating temperature devices.

LWIR QDIPs with operation temperature higher than 200 K were demonstrated. Devices with two different confinement enhancing layers were studied. With proper device parameters, we are able to achieve high responsivity and high operating temperature at the same time. Despite dramatic differences in their device characteristics, both LWIR CE-DWELL devices can be operated at high temperature. The device with better performance at lower temperatures does not necessarily have better performance at elevated temperatures. Better suppression of the dark current is essential for the high-temperature operation QDIPs.

References

[1] J. Phillips, "Evaluation of the fundamental properties of quantum dot infrared detectors," *J. Appl. Phys.*, vol. 91, pp. 4590–4594, 2002.

[2] S. Y. Wang, S. D. Lin, H. W. Wu, and C. P. Lee, "High performance InAs/GaAs quantum dot infrared photodetectors with AlGaAs current blocking layer," *Infrared Phys. Technol.*, vol. 42, pp. 473–477, 2001.

[3] S. Y. Wang, M. C. Lo, H. Y. Hsiao, H. S. Ling, and C. P. Lee, "Temperature dependent responsivity of quantum dot infrared photodetectors," *Infrared Phys. Technol.*, vol. 50, pp. 166–170, 2007.

[4] S. Chakrabarti, A. D. Stiff-Roberts, P. Bhattacharya, S. Gunapala, S. Bandara, S. B. Rafol, and S. W. Kennerly, "High-temperature operation of InAs–GaAs quantum-dot infrared photodetectors with large responsivity and detectivity," *IEEE Photon. Technol. Lett.*, vol. 16, no. 5, pp. 1361–1363, May 2004.

[5] L. Jiang, S. S. Li, N. T. Yeh, J. I. Chyi, C. E. Ross, and K. S. Jones, "$In_{0.6}Ga_{0.4}As$/GaAs quantum-dot infrared photodetector with operating temperature up to 260 K," *Appl. Phys. Lett.*, vol. 82, pp. 1986–1988, 2003.

[6] P. Bhattacharya, X. H. Su, S. Chakrabarti, G. Ariyawansa, and A. G. U. Perera, "Characteristics of a tunneling quantum-dot infrared photodetector operating at room temperature," *Appl. Phys. Lett.*, vol. 86, p. 191106, 2005.

[7] H. Lim, S. Tsao, W. Zhang, and M. Razeghia, "High-performance InAs quantum-dot infrared photodetectors grown on InP substrate operating at room temperature," *Appl. Phys. Lett.*, vol. 90, p. 131112, 2007.

[8] E. T. Kim, A. Madhukar, Z. Ye, and J. C. Campbell, "High detectivity InAs quantum dot infrared photodetectors," *Appl. Phys. Lett.*, vol. 84, pp. 3277–3279, 2004.

[9] S. Krishna, "Quantum dots-in-a-well infrared photodetectors," *Infrared Phys. Technol.*, vol. 47, pp. 153–163, 2005.

[10] G. Ariyawansa, A. G. U. Perera, G. S. Raghavan, G. von Winckel, A. Stintz, and S. Krishna, "Effect of well width on three-color quantum dots-in-a-well infrared detectors," *IEEE Photon. Technol. Lett.*, vol. 17, no. 5, pp. 1064–1066, May 2005.

[11] S. D. Gunapala, S. V. Bandara, C. J. Hill, D. Z. Ting, J. K. Liu, S. B. Rafol, E. R. Blazejewski, J. M. Mumolo, S. A. Keo, S. Krishna, Y. C. Chang, and C. A. Shott, "640 × 512 pixels long-wavelength infrared (LWIR) quantum-dot infrared photodetector (QDIP) imaging focal plane array," *IEEE J. Quantum Electron.*, vol. 43, no. 3, pp. 230–237, Mar. 2007.

[12] X. Lu, J. Vaillancourt, and M. J. Meisner, "Temperature-dependent photoresponsivity and high-temperature (190 K) operation of a quantum dot infrared photodetector," *Appl. Phys. Lett.*, vol. 91, p. 051115, 2007.

[13] H. S. Ling, S. Y. Wang, C. P. Lee, and M. C. Lo, "High quantum efficiency dots-in-a-well quantum dot infrared photodetectors with AlGaAs confinement enhancing layer," *Appl. Phys. Lett.*, vol. 92, p. 193506, 2008.